Journal of Modern Science and Technology
Vol. 1. No. 1. May 2013 Issue. Pp.52-60

Experimental and Numerical Investigation of Flow over a Cylinder at Reynolds Number 10^5

Toukir Islam and S.M. Rakibul Hassan

Flow past a stationary circular cylinder at $Re=10^5$ is studied numerically using Favre-averaged Navier-Stokes equation and solved via finite volume method. Numerical observations are compared with experimental results and with research works of other researchers. Different flow phenomena such as flow separation, pressure distribution over the surface, drag, vortex shedding etc. are also studied at different boundary conditions. A brief comparison between the 2D and 3D numerical calculations as well as the nature of vorticity distribution and effect of surface roughness are extensively studied. In case of smooth cylinder, the separation angles for 2D or 3D numerical calculation are found to be around 80~90° in either side of the cylinder from the upstream stagnation point. The drag coefficients for smooth surface are 0.771 and 0.533 for 2D and 3D numerical calculation respectively and subsequent changes in drag due to introducing surface roughness are demonstrated. The critical surface roughness is found to be around 0.004 with coefficient of drag 0.43. Though the wake structure was vaguely visible, they are not as periodic as in Karman street.

Field of research: Mechanical Engineering.

Keywords: Separation, Coefficient of drag, Relative surface roughness, Karman Vortex street.

1. Introduction

Owing to geometric simplicity and widespread applications in real life, the flow past a circular cylinder has been extensively studied. Despite its simple shape, the flow past a circular cylinder produces several flow features associated with more complex geometries. Theoretical flow over a cylinder is considered to be inviscous, incompressible and irrotational; known as 'Potential Flow' in which the reattachment of streamlines is considered to be complete and symmetrical to detachment at the upstream resulting in zero drag and lift force. In real life, zero lift force is quite acceptable, but there must be a force on the body towards the flow direction i.e. more or less, drag is present in case of flow over the body. There is presence of viscosity and the flow is neither incompressible nor irrotational. Avoidance of the term viscosity in early era of fluid dynamics led to a paradox called 'D'Alembert's paradox' that remained as mystery for about one and half centuries until Ludwig Prandtl suggested the presence of thin viscous boundary layer in 1904. The variation of flow phenomena can de described with respect to Reynolds number as the fluid flow exhibits similar behavior within a particular range of Reynolds number. The trend of behavioral change also follows the change of Reynolds number.

Toukir Islam, Bangladesh University of Engineering and Technology (BUET), Bangladesh.
Email: toukir.buet07@gmail.com
S.M. Rakibul Hassan, Bangladesh University of Engineering and Technology (BUET). Bangladesh.
Email: rakibulhassan21@gmail.com

This paper is subjected to both numerical and experimental investigation of air flow over a circular cylinder of 3 inch diameter at a definite Reynolds number 10^5. Dealing with a particular Reynolds number flow allows us to fix an important variable which is Reynolds number itself and concentrate on other important parameters for analysis while flow characteristics remain same. The numerical procedure includes both 2D and 3D simulation for different relative roughness (ratio of surface roughness to diameter of the cylinder). Favre averaged Navier-Stokes equations are used along with finite volume scheme to solve these equations over the computational domain. Experimental procedure is carried out in a wind tunnel with a plastic cylinder of 3 inch diameter having a pressure tap on the surface. Numerical procedure is implied for predicting the point of separation i.e. separation angle on both the top and bottom surfaces at zero relative roughness by predicting the instability of coefficient of pressure C_P at the surface of the cylinder as C_P tends to fluctuate frequently with in the separated zone. Coefficient of drag C_D is another important dimensionless parameter whose relative fluctuation is observed under different surface roughness which can be used to predict the critical relative roughness for flow over the cylinder at the Reynolds number 10^5. The vorticty distribution over and along the length over the cylinder was also observed. Experimental procedure is limited to measure C_P at different angular position on the surface of the cylinder to predict the separation angle and overall drag of the cylinder at Reynolds number 10^5.

2. Literature Review:

The flow phenomena for flow over the stationary cylinder of fixed dimension depend on the free stream velocity and other conditions such as flowing fluid density, surface roughness etc. Anderson (2010, p. 274) described the rejoins of different flows with respect to bands of Reynolds number. For flow in the region of $0< Re<4$, streamlines are reattached similar way as they were detached resulting in near balance of pressure at upstream and downstream, known as 'Stokes flow'. $4<Re<40$ region exhibits separation and wakes symmetrical to the flow axis. Above Re=40, the flow becomes unstable; vortices which were in fixed position starts to shed alternately in a regular fashion resulting in 'Von Karman vortex street'. With increasing Re, the Karman vortex street becomes turbulent and begins to metamorphose into distinct wake. The laminar boundary layer on the cylinder separates from the surface on the forward face. In this region of $10^3<Re<3\times10^5$, the transition of boundary layer from laminar to turbulent occurs with subsequent reduction of drag coefficient. At a definite Re, the drag coefficient becomes minimum. This phenomenon is known as 'Drag Crisis' and the Re at which it occurs is known as critical Reynolds number, Re_c. Re higher than the Re_c exhibits increase in C_D as the wake becomes flatter at downstream that increases pressure drag. Willamson (1996) has provided comprehensive description of flow phenomena at different Reynolds number. Fornberg (1980), Wu et al. (2004), Sen et al. (2010) have described separation angle for flow over the cylinder at low Reynolds number. Though their works do not cover the middle ranged or higher Reynolds number, procedures to find the separation angle are described vividly. Singh and Mittal (2005) studied flow past a circular cylinder for Re= 100 to 10^7 numerically by solving the unsteady incompressible two dimensional Navier-Stokes equations via a stabilized finite element formulation and they described the shear layer instability and drag crisis phenomena briefly. Selvam (1997) presented his results for two dimensional Large Eddy Simulation (LES) for

flow past a cylinder and observed reduction in C_D with increasing Reynolds number; though in different extend from Singh and Mittal. Effect of relative roughness on flow over circular cylinder is observed by Achenbach and Heinecke (1981) in the range of Reynolds number 6×10^3 to 5×10^6 as they investigated vortex shedding phenomena in this range. Mittal and Balachander (1995) described the effect of three-dimensionality on the lift and drag of nominally two-dimensional cylinders which is useful to describe the variation of numerical results between two dimensional and three dimensional analysis. Adachi (1995) described effect of surface roughness for flow over a body at high Reynolds number using cryogenic wind tunnel.

3. Methodology:

3.1 Numerical Procedure:

Numerical flow simulation is performed by solving Navier-Stokes equations, which are formulation of mass, momentum and energy conservation laws. To predict turbulent flows, the Favre-averaged Navier-Stokes equations are used, where time averaged effects of the flow turbulence on the flow parameters are considered. The conservation laws for mass, angular momentum and energy in the Cartesian coordinate system rotating with angular velocity Ω about an axis passing through the coordinate system's origin can be written in the conservation form as follows (SolidWorks Flow Simulation 2012):

$$\frac{\partial \rho}{\partial t} + \frac{\partial(\rho u_i)}{\partial x_i} = 0$$

$$\frac{\partial(\rho u_i)}{\partial t} + \frac{\partial(\rho u_i u_j)}{\partial x_j} + \frac{\partial \mathrm{P}}{\partial x_i} = \frac{\partial}{\partial x_i}\left(\tau_{ij} + {\tau_{ij}}^R\right) + S_i$$

$$\frac{\partial(\rho H)}{\partial t} + \frac{\partial(\rho u_i \mathrm{H})}{\partial x_i} = \frac{\partial}{\partial x_i}\left[u_j\left(\tau_{ij} + {\tau_{ij}}^R\right)\right] + \frac{\partial \rho}{\partial t} + S_i u_i - {\tau_{ij}}^R \frac{\partial u_i}{\partial x_i} + \rho\varepsilon$$

$$H = \frac{u^2}{2}$$

Here u is fluid velocity, ρ is fluid density, S_i is a mass-distributed external force per unit mass due to porous media resistance , a buoyancy (- ρg_i), and the coordinate system's rotation, τ_{ij} is the viscous shear stress tensor, ${\tau_{ij}}^R$ is Reynolds-stress tensor. The subscripts are used to denote summation over the three coordinate directions. *k-ε* turbulence model is used for the turbulent kinetic energy and its' dissipation rate. No slip conditions and adiabatic wall conditions are applied. Computational domain of 22″×16″×13″ was used for calculation for cylinder of 3″ diameter. No heat generation or transfer is considered.

The cell-centered finite volume (FV) method is used to obtain conservative approximations of the governing equations on the locally refined rectangular mesh. The governing equations are integrated over a control volume which is a grid cell, and then approximated with the cell-centered values of the basic variables. The integral conservation laws may be represented in the form of the cell volume and surface integral equation:

$\frac{\partial}{\partial t}\int \mathbf{U}\,\mathrm{dv} + \oint F.ds = \int Q dv$, which is replaced by $\frac{\partial}{\partial t}(U\mathrm{v}) + \sum_{cell\ faces} F.s = Qv$

The second-order upwind approximations of fluxes F are based on the implicitly treated modified Leonard's QUICK approximations (Roache 1998) and the Total Variation Diminishing (TVD) method (Hirsch 1988).

3.2 Experimental Procedure:

Fluid mechanics Lab facilities of Bangladesh University of Engineering and Technology (BUET) was used to study the flow over the cylinder experimentally. The set-up wind tunnel consists of two induced fans, adjusting damper to control flow, pitot tubes and pressure tapping arrangements for inclined manometer (manometric fluid is water). A hollow cylinder of 3 inch dia; placed across the wind tunnel was subjected to the flow which had a pressure tapping on its surface. The cylinder was rotated on its own axis and angle indicator on the face of the cylinder was used to indicate the position of the pressure tap; thus the rotation angle. Two pitot tubes were used; one on the upstream and another on the downstream of the flow. Each pitot tube had an adjacent pressure tap. Pitot tubes could be moved vertically to take reading at different vertical positions. Now if h_m is manometric deflection and ρ_m, ρ_a are the density of manometric fluid and air respectively, then the free stream velocity

$$V_\infty = \sqrt{\frac{2g\times\ hm\times\ \rho m}{\rho a}}$$

If we want the flow of a definite Reynolds number, we just have to set h_m accordingly. Here $h_m = (h_2 - h_1)$. Now the difference between the free steam static pressure and the pressure on the surface of the cylinder is $(h_5 - h_1)$ and the free stream dynamic pressure is $(h_2 - h_1)$; we can defy Cp as

$$Cp = \frac{(h5 - h1)}{(h2 - h1)}$$

$(h_2 - h_1)$ remains constant for a Reynolds number and measured once. So, several readings of $(h_5 - h_1)$ are taken by rotating the cylinder anti clockwise direction from 0° to 350°; 10° for each rotation. The coefficient of drag is measured by the area under the curve Cp vs sinθ.

Fig 1: Schematics of Experimental Setup

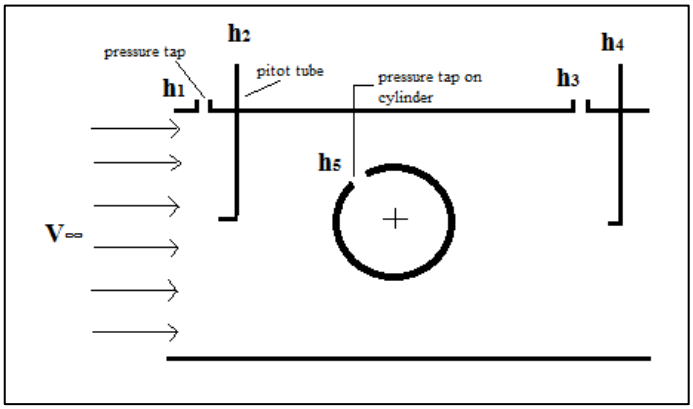

4. Results and Discussions:

2D and 3D numerical calculations at zero roughness, 2D numerical calculations at various roughness and experimental calculation, all at Re=10^5 are done here. Fig 2 represents the variation of C_P with respect to angular position θ of the stationary

cylinder. Here θ is taken anti-clockwise direction from the upstream stagnation point. We know that, at the onset of separation, C_P becomes unstable. The angle at which the separation occurs is known as separation angle. Separation angle on the upper and lower surface of the cylinder shoulder can de denoted as θ_{SU} and θ_{SL} respectively. The separation angles at different numerical and experimental calculations are presented in the table 1 and the observations are based on Fig 2. A secondary local suction peak on the surface of the cylinder at an angle around 315 degree for experimental C_P is observed. Singh and Mittal (2005) observed similar suction peak at $Re=10^5$ and concluded that the peaks occur beyond the shoulder of the cylinder and points to the presence of a local recirculation zone close to the surface.

Fig 2: Distribution of C_P at Different Angular Position on the Cylinder Surface.

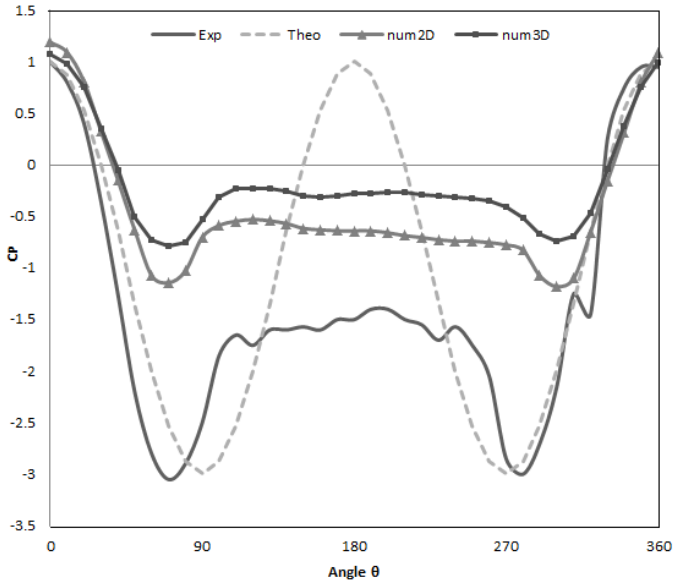

Table 1: Separation Angle

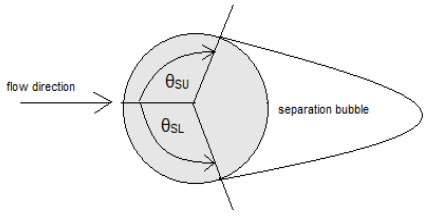

	Angle (in degree)	Numerical (smooth surface)		Experimental
		2D	3D	
	θ_{SU}	80	80	100
	θ_{SL}	90	100	100

We observe asymmetrical separation at upper and lower surfaces. Now the C_D for 2D and 3D calculations for smooth surface is found to be 0.771 and 0.553 respectively. As we see, the C_D for 2D calculation is bit over predicted. Mittal and Balachander (1995) observed the similar results and concluded that the higher value of drag coefficient in 2D simulation is caused due to higher level of Reynolds stresses resulting in a shorter formation length behind the bluff body. Now C_D for experimental results derived from the area under the curve C_P Vs. sinθ (Fig 3) is

1.96. This result is well over-predicted compared to experimental result of Achenbach (1968) which is around 1.06. Probable reason for the deviation is the difference in surface roughness. Fig 4 shows the change of C_D at $Re=10^5$ with respect to different relative surface roughness for 2D numerical calculations. Relative surface roughness is the ratio of roughness to the diameter of the cylinder and denoted as K_S/D. For example, for roughness 300 micrometer of a cylinder of 0.0762 meter diameter, relative surface roughness will be 0.00394. From the figure, it is evident that, the C_D decreases with increasing K_S/D up to a certain K_S/D; where it is minimum and after that, the C_D increases with increasing roughness. The relative roughness at which the C_D is minimum can be noted as critical roughness, $(K_S/D)_C$. Achenbach and Heinecke (1981) suggested that the critical Reynolds number i.e.

Reynolds number at which the C_D becomes minimum for the flow over the cylinder at different Re; decreases with increasing surface roughness and the C_D at the critical Reynolds number increases with increasing roughness. In case of 2D numerical calculation at $Re =10^5$, the $(K_S/D)_C$ is found to be 0.003937008 and C_D at that point is around 0.43.

From the velocity contour representation (Fig 5(a),5(b)) for both 2D and 3D numerical calculations for smooth surface, the wake structures are visible but they are not as well organized and periodic as in Karman street at lower subcritical (Fig 5(c)) Reynolds number. Wakes are narrower resulting in much delayed separation. The unstable shear layer is much closer to the point of separation. Asymmetric vorticity distribution also observed from Fig 6 that results in variation of force towards axial direction (z direction).

Fig 3: C_P Vs. sinθ at Re 10^5 (experimental)

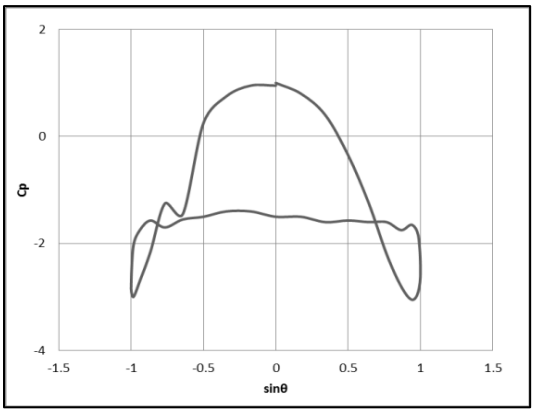

Fig 4: C_D at Different Ks/D

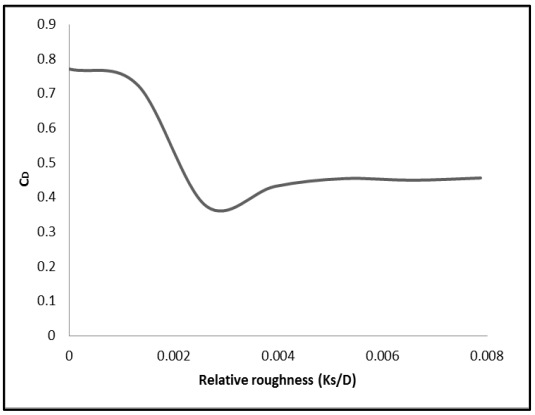

Fig 5: Velocity Contours (A) Re 10^5, 2D Simulation (B)Re 10^5, 3D Simulation (C)Re 67, 2D Simulation

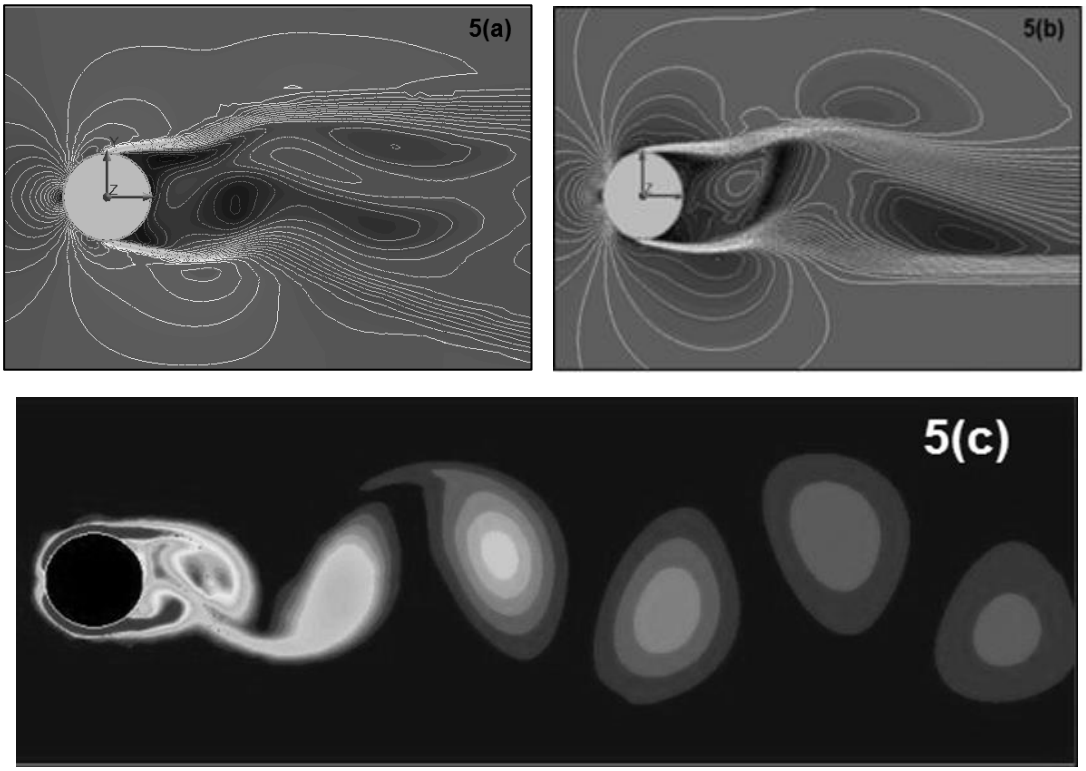

Fig 6: Vorticity Distribution Visible from the Top View of the Cylinder at (A) Center Plane, (B) 0.02 Meter Offset from Center Plane, (C) 0.04 Meter Offset from Center Plane.

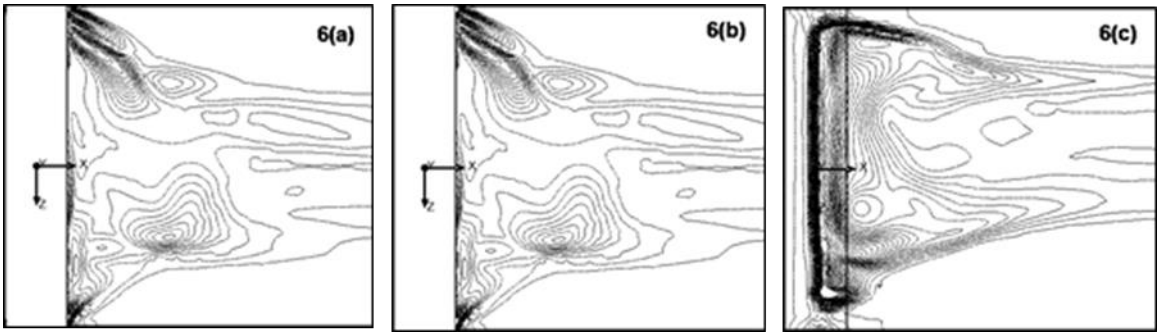

5. Conclusion:

Flow over the stationary cylinder is studied at a subcritical Re= 10^5 through experiments and numerical calculations using finite volume method to solve Navier-Stokes equations. Though 2D numerical calculation is vital to predict drag crisis phenomena and shear layer instability, 3D numerical calculation provides us the overall idea about the real flow phenomena. Surface roughness and turbulence intensity controls the nature of the flow over a bluff body. In this article, the effect of

surface roughness on drag coefficient and shift of critical Reynolds number due to relative roughness are illustrated through 2D numerical calculations. For a definite relative roughness, transition of boundary layer occurred at Re as low as 10^5. Vorticity distribution in parallel and perpendicular to flow directions found to be asymmetrical that may cause vibration and lift or drag force. There are certain areas those worth attentions from future researchers. The experimental section was covered for cylinder of certain surface roughness and different surface roughness would be implied to study the effect of surface roughness on flow parameters experimentally. The effect of surface roughness on the separation angle can be another center of interest for future researchers.

References:

Tsutomu, A. (1995), 'The Effect of Surface Roughness of a Body in the High Reynolds Number Flow', *International Journal of Rotating Machinery*, 1 (3-4), 187-197.

Achenbach, E. (1968), 'Distribution of local pressure and skin friction around a circular cylinder in cross-flow up to Re = 5× 10^6', *Journal of Fluid Mechanics,* 34, 625-639.

Achenbach, E., and Heinecke, E. (1981), 'On vortex shedding from smooth and rough cylinders in the range of Reynolds numbers 6 ×10^3 to 5 ×10^6', *Journal of Fluid Mechanics*, 109, 239-251.

Tsutomu, A. (1995), 'The Effect of Surface Roughness of a Body in the High Reynolds Number Flow', *International Journal of Rotating Machinery*, 1 (3-4), 187-197.

Anderson, J. D. (2010)*, Fundamental of Aerodynamics [In SI unit]*, 5th ed, Tata McGraw Hill Education Private Limited, New Delhi.

Fornberg, B. (1980), 'A numerical study of steady viscous flow past a circular cylinder', *Journal of Fluid Mechanics*, 98, 819-855.

Hirsch, C. (1988), *Numerical computation of internal and external flows*, John Wiley and Sons, Chichester.

Mittal, R., and Balachander, S. (1995), 'Effect of three-dimensionality on the lift and drag of nominally two-dimensional cylinders', *Physics of Fluids*, 7, 1841- 1865.

Roache, P.J. (1998), '*Technical Reference of Computational Fluid Dynamics'* Hermosa Publishers, Albuquerque, New Mexico, USA. Edition Missing

Sen, S., Mittal, S., and Biswas, G. (2010), 'Numerical Simulation of Steady Flow Past a Circular Cylinder', *Proceedings of the 37th National & 4th International Conference on Fluid Mechanics and Fluid Power*, IIT Madras, December 16-18. Chennai, India.

Selvam, R.P. (1997), 'Finite element modeling of flow around a circular cylinder using LES'., Journal of Wind Engineering and Industrial *Aerodynamics*, 67 & 68, 129-139.

Singh, S.P., and Mittal, S. (2005), 'Flow Past a Cylinder: Shear Layer Instability and Drag Crisis', *International Journal for Numerical Methods in Fluids*, 47, 75—98.

Technical Reference (2012), SolidWorks Flow Simulation, SolidWorks.

Williamson, C.H.K. (1996), 'Vortex Dynamics in the Cylinder Wake', *Annual Review of Fluid Mechanics*, 28, 477-539.

Wu, M..H., Wen, C.Y., Ten, R.H., Weng, M.C., and Wang, A.B. (2004), 'Experimental and numerical study of the separation angle for flow around a circular cylinder at low Reynolds number', *Journal of Fluid Mechanics*, 515, 233-260.